

Dual Nature of Magnetism Driven by Momentum Dependent f - d Kondo Hybridization

Byungkyun Kang,^{1,*} Yongbin Lee,² Liqin Ke,² Hyunsoo Kim,³ and Myoung-Hwan Kim⁴

¹College of Arts and Sciences, University of Delaware, Newark, DE 19716, USA

²Ames Laboratory, U.S. Department of Energy, Ames, IA, 50011, USA

³Department of Physics, Missouri University of Science and Technology, Rolla, 65409, MO, USA

⁴Department of Physics and Astronomy, Texas Tech University, Lubbock, Texas 79409, USA

Intricate nature of magnetism in uranium-based Kondo lattices is a consequence of correlations between U-5 f and conduction electrons. Using linearized quasiparticle self-consistent GW plus dynamical mean-field theory, we demonstrate a crossover from incoherent to coherent f - d Kondo cloud in the paramagnetic phase of UTe₂ with reduced volumes, USbTe and USbSe. As the transition occurs, we observe an augmented f - d coherence and Pauli-like magnetic susceptibility, with a substantial frozen magnetic moment of U-5 f persisting. We show that momentum dependent f - d hybridization is responsible for the magnetic moments arising from the renormalized f electrons' van Hove singularity. Our findings provide a unique perspective to explain the dual nature of magnetism and the long-range magnetic ordering induced by pressure in UTe₂.

Bewildering behavior of U-5 f electrons in uranium-based compounds, extending from localisation to mobility and dualism [1–3], is further perplexed by Kondo screening by conduction electrons, leading to the advent of unprecedented phenomena in a variety of Kondo lattices. Amorese et al.[3] elucidated the dual nature of local atomic-like multiplet states in Pauli-paramagnetic UFe₂Si₂, which has been known to exhibit Kondo-like behaviour at low temperatures [4]. USbTe, a Kondo lattice ferromagnet, has been found to possess a large anomalous Hall conductivity, which is suggested to be due to the intrinsic Berry curvature hosted by the Kondo hybridization between the local magnetic moment of U-5 f and the conduction electrons [5]. UTe₂, a heavy fermion superconductor, has been reported to lack long-range magnetic ordering [6], in contrast to other uranium compounds, such as USbTe and USbSe ($T_C \sim 127$ K) [7]. Nonetheless, UTe₂ has been found to exhibit pressure-induced long-range magnetic ordering [8–11]. Li et al. [9] demonstrated that increasing pressure leads to a diminution of magnetic moments and long-range magnetic ordering. The manifestly disparate behaviours exhibited in U-5 f systems reflect a profound bond between U-5 f and its surroundings, and are not easily explicable by existing theories.

Theoretical studies have proposed the presence of orbital-selective Mott phases (OSMP) to explain the duality observed in multi-band correlated systems [12–14]. This phenomenon is characterized by the coexistence of localized electrons in certain orbitals and itinerant electrons in other orbitals. The OSMP has been employed to explain the dual nature of Fe-based compounds. For example, Kim et al. [15] reported that the Mott transition in FePS₃ can be orbital selective, with the t_{2g} states undergoing a correlation-induced insulator-to-metal transition while the e_g states remain gaped under pressure. However, no evidence of the occurrence of the OSMP has been found in the 5 f system.

Unlike 4 f electrons in the lanthanide elements, which are typically localized within the Mott physics [16], the degree of localization of 5 f electrons in the actinide elements is

strongly dependent on the crystal structure [1], crystal electric field, and spin-orbit coupling (SOC). These factors can affect the hybridization channels, leading to a varying screening of the U-5 f magnetic moments [17], thereby altering the magnetization mechanism depending on whether Kondo hybridization is coherent or incoherent. According to the multichannel Kondo model [18, 19], Kondo systems can be classified into three types (under, fully, over-screened) based on the local magnetic moment raised by impurity spin S and the number of conduction electron channels, n . In the under-screened case ($n < 2S$), S is partially screened at low temperatures, potentially allowing for long-range magnetic ordering due to the Ruderman Kittel-Kasuya-Yosida (RKKY) interaction. An example of this is the Anderson lattice model of uranium monochalcogenides, where UTe is modelled with $S = 1$ and $n < 2$ [20, 21]. However, the RKKY mechanism may not be applicable to coherent U-5 f Kondo lattices, as the Kondo coupling and the RKKY interaction favor different ground states [22, 23].

In a Bloch electrons system, van Hove singularity (VHS) [24] can be attributed as a source of magnetisation. As the Fermi energy approaches a VHS of the electronic density of states (DOS), the DOS diverges, allowing for weak interactions to have a significant influence on the electronic behavior. This can result in instabilities in charge and spin susceptibilities, leading to substantial enhancement of ferromagnetism [25, 26] and antiferromagnetism [27]. The VHS has been associated with the local magnetic moment in a transition metal [28] and graphene bilayer [29]. By using density functional theory (DFT) combined with dynamical mean field theory (DMFT), Hausoel et al. [28] recently investigated the paramagnetic phase spectrum of Ni metal. Their results revealed a van Hove magnet at the L point of the Brillouin zone, characterized by a large effective mass and temperature-dependent magnetic susceptibility. This feature has not been previously observed in U-5 f Kondo lattice.

In this work, we scrutinized the alteration from disordered to ordered f - d Kondo hybridization in the paramagnetic phase of Kondo lattices of UTe₂, UTe₂ with reduced volume, USbTe and USbSe. We discovered that UTe₂ with reduced volume and USbSe are in the coherent regime, exhibiting Pauli-like magnetic susceptibility and dispersive bands arising from the

* bkang@udel.edu

hybridization of U-6d and renormalized U-5f electrons. This leads to delocalized U-5f electrons, i.e. Bloch-like quasiparticle states, and a remarkably significant U-5f magnetic moment. We ascribed this duality of Pauli-like magnetic susceptibility and local magnetic moments to momentum reliant coherent *f-d* hybridization, with the VHS being the origin of the magnetic moment. This feature was employed to investigate the emergence of long-range magnetic ordering in UTe₂ under pressure.

Coulomb interaction tensor. The crystal structures of the

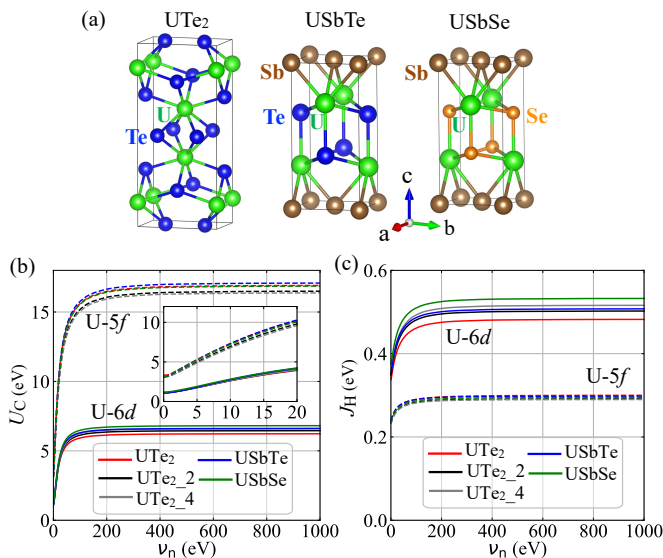


FIG. 1. (a) Crystal structure of UTe₂, USbTe, and USbSe. Calculated onsite (b) Coulomb interaction U_C and (c) exchange interaction J_H for U-5f and U-6d with inclusion of SOC as a function of $\nu_n = 2n\pi/\beta$ bosonic frequencies. In (b), inset shows magnified views of U_C in low frequency range.

orthorhombic phase (Immm) UTe₂ [30] and the tetragonal phase (P4/nmm) USbTe and USbSe [31] are depicted in Fig. 1 (a). To investigate the impact of pressure on the electronic structure of UTe₂, structures with a decreased volume of UTe₂ were generated by reducing the experimental lattice parameters [30] by 2 % (UTe_{2_2}) and 4 % (UTe_{2_4}). The constrained random phase approximation [32] was employed to calculate the onsite Coulomb interaction U_C and exchange interaction J_H , for U-5f and U-6d orbitals, taking into account SOC. Fig. 1 (b) and (c) show that both U_C and J_H increase and reach their unscreened values at high frequencies. The static U_C of U-6d and U-5f orbitals were found to be comparable across the compounds studied. However, U_C of U-5f is larger than that of U-6d, while J_H for U-5f is smaller than that of U-6d.

Electronic structures. The local self-energies of U-5f and U-6d were determined by solving two distinct single impurity models using the continuous time quantum Monte Carlo method within the framework of DMFT [33]. The dynamic Coulomb interaction tensors of U-5f and U-6d were employed in this process. By eliminating the off-diagonal elements in the hybridization functions, the local self-energy

is assumed to be diagonal in the spherical harmonics basis. Supplementary Figure 1 (Fig. S1) demonstrates that the off-diagonal elements are relatively small and insignificant. Further details of the methods used can be found in the supplementary materials. The electron occupancies of U-5f and U-6d orbitals at 300 K are presented in Table I. The U-6d orbitals were found to have a spread occupation across all *d* orbitals, while the U-5f orbitals were split into $j = 5/2$ and $j = 7/2$ multiplets, with a significant occupation of the $j = 5/2$ multiplet. The total occupations of U-5f orbitals were 2.27, 2.25, 2.26, 2.24, and 2.31 for UTe₂, UTe_{2_2}, UTe_{2_4}, USbTe, and USbSe, respectively. The U-5f occupation for UTe₂ was found to be in accordance with the measured $5f^2$ configuration [34], indicating a substantial local magnetic moment of U-5f and the presence of an orbital selective Kondo effect [35].

Figure 2 presents the calculated spectral functions and atomic-orbital projected DOS. It is observed that all compounds share a common property of a strong U-5f peak in the vicinity of the Fermi level at low temperature. The temperature dependence of the U-5f peak between 150 K and 1000 K is consistent with that of the U-6d peak, indicating hybridization between U-5f and U-6d. In contrast, the DOS of other anions of Te, Sb, and Se are small and their temperature dependence are subtle. Furthermore, the presence of flat *f* bands and kink-like band structures implies that *f-d* Kondo hybridization governs the electronic structure in the vicinity of the Fermi level [16, 35, 36]. This is in agreement with the experimental observation of Kondo lattice in UTe₂ [37], USbTe [5, 38], and USbSe [38]. The calculated Kondo hybridization of USbTe with respect to temperature was found to be in agreement with angle-resolved photoemission spectroscopy (ARPES) measurements [5]. Similarly, the dispersive Kondo resonance peaks near the Fermi level of UTe₂ were also observed in the ARPES [39].

Crossover from incoherent to coherent. The local total angular momentum susceptibility, χ_{J_Z} , was calculated as $\int_0^\beta d\tau \langle J_z(\tau) J_z(0) \rangle$. Fig. 3 (a) highlights the χ_{J_Z} of U-5f for UTe₂, which exhibits a Curie-like behavior. Upon decreasing the volume, UTe_{2_4} exhibits Pauli-like behavior of weak temperature dependence, while USbTe and UTe_{2_2} display an intermediate susceptibility. USbSe, on the other hand, shows Pauli-like behavior. At temperatures between 150 and 250 K, a flat χ_{J_Z} was observed for USbSe which clearly shows in Fig. 3(b) both experiment and theory. These results suggest that the magnetic moment on UTe₂ is strong and resilient, while in USbSe and UTe_{2_4}, the electrons from the *s*, *p*, *d* and *f* orbitals of neighboring atoms are arranged in an antiparallel manner to the moment of U-5f, resulting in the cancellation of net moments [41].

Comparison of χ_{J_Z} with experiments [7, 40] yielded good agreement, as demonstrated in Fig. 3(b). The inverse of the calculated $\chi = g\chi_{J_Z}k_B/3$ is presented, where g is set to 0.8 [2, 42]. The calculated χ^{-1} of UTe₂, USbTe, and USbSe is found to be in the order of UTe₂ < USbTe < USbSe, which is consistent with the experimental χ^{-1} when a magnetic field is applied along the b axis ($H \parallel b$). The slope of linear χ^{-1} of UTe₂ is confirmed by both experimental and

TABLE I. Calculated electron occupation of U-5*f* and U-6*d* orbitals in UTe₂, USbTe, and USbSe at $T = 300$ K. U-5*f* and U-6*d* orbitals are labelled for convenience in this work.

j	U-5 <i>f</i>														U-6 <i>d</i>									
	5/2						7/2								3/2				5/2					
j_z	-2.5	-1.5	-0.5	0.5	1.5	2.5	-3.5	-2.5	-1.5	-0.5	0.5	1.5	2.5	3.5	-1.5	-0.5	0.5	1.5	-2.5	-1.5	-0.5	0.5	1.5	2.5
label	f_1	f_2	f_3	f_4	f_5	f_6	f_7	f_8	f_9	f_{10}	f_{11}	f_{12}	f_{13}	f_{14}	d_1	d_2	d_3	d_4	d_5	d_6	d_7	d_8	d_9	d_{10}
UTe ₂	0.37	0.31	0.36	0.36	0.30	0.36	0.03	0.03	0.03	0.03	0.03	0.03	0.03	0.03	0.21	0.23	0.23	0.21	0.17	0.19	0.19	0.19	0.19	0.17
UTe ₂₋₂	0.35	0.30	0.36	0.35	0.30	0.35	0.03	0.03	0.03	0.03	0.03	0.03	0.04	0.03	0.21	0.22	0.22	0.21	0.17	0.17	0.19	0.19	0.17	0.17
UTe ₂₋₄	0.35	0.27	0.33	0.34	0.27	0.34	0.04	0.04	0.05	0.05	0.05	0.05	0.04	0.04	0.21	0.23	0.23	0.21	0.18	0.18	0.20	0.20	0.17	0.18
USbTe	0.34	0.34	0.33	0.33	0.35	0.35	0.03	0.03	0.03	0.03	0.03	0.03	0.03	0.03	0.23	0.22	0.22	0.23	0.18	0.17	0.18	0.18	0.17	0.18
USbSe	0.34	0.35	0.33	0.33	0.36	0.35	0.04	0.03	0.03	0.04	0.04	0.03	0.04	0.04	0.20	0.20	0.20	0.20	0.15	0.16	0.17	0.17	0.16	0.15

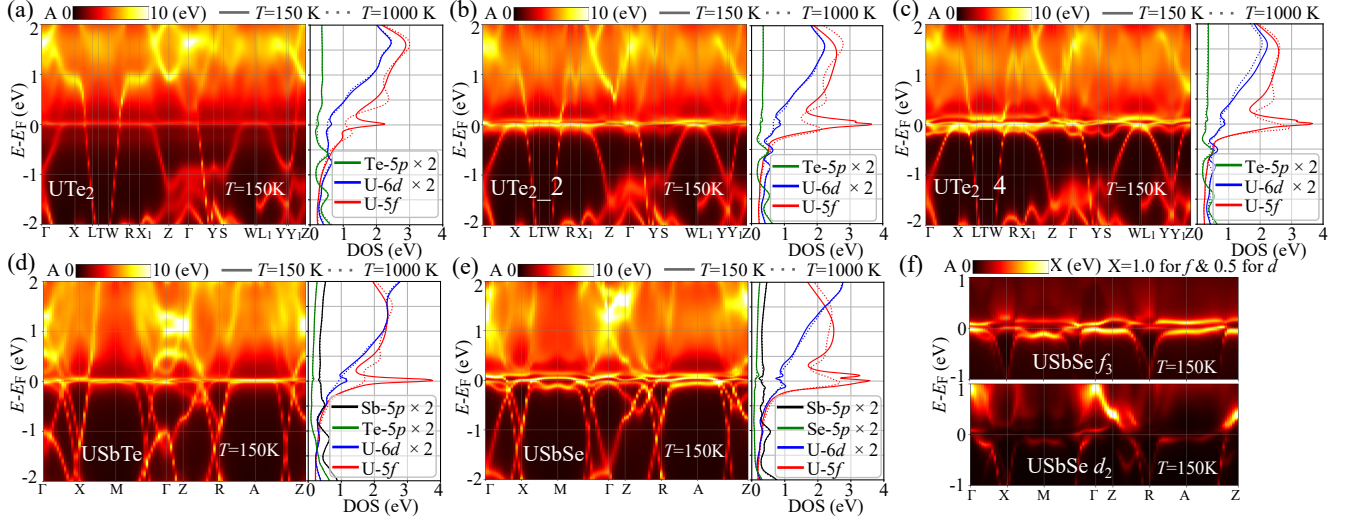


FIG. 2. Calculated spectral functions and DOS for (a) UTe₂, (b) UTe₂₋₂, (c) UTe₂₋₄, (d) USbTe, (e) USbSe. (f) Orbital projected spectral functions for USbSe. f_3 (d_2) projected spectral function is presented in upper (lower) panel (see the orbital labeling in Table I). In the top of each figure, A denotes spectral weight.

theoretical results. For USbTe, both experiment (H||b) and theoretical calculations show a linear χ^{-1} down to 150 K, albeit with a slightly different slope. Experiment χ^{-1} (H||b) of USbSe exhibits Pauli-type behavior from approximately 140 to 190 K, followed by Curie-like behavior at higher temperatures. Our calculations further suggest Pauli-type behavior from 150 to 250 K, albeit with a slightly different temperature scale. This implies that USbSe is in the coherent regime with Pauli-type behavior at low temperatures, corroborated by both theory and experiment.

The local angular momentum correlation functions $\chi_{J_z}(\tau) = \langle J_z(\tau)J_z(0) \rangle$ are presented in Fig. 3 (c). The correlation function can be used to assess the degree of magnetic moment localization [43]. The instantaneous J values of U⁴⁺ range from 4.4 to 4.1, which is consistent with the ³H₄ Russell Saunders ground state configuration [42]. Fig. S2 shows that the charge susceptibility $\chi_N = \int_0^\beta d\tau \langle N(\tau)N(0) \rangle$ of U-5*f* electrons is enhanced in the coherent regime, while the $\chi_{J_z}(\tau)$ is reduced, as illustrated in Fig. 3 (c). These indicate that the itinerant character of the U-5*f* electrons in USbSe and UTe₂₋₄ is significantly enhanced, as further evidenced by the diverg-

ing hybridization functions in these materials, as shown in Fig. S3. Remarkably, USbSe and UTe₂₋₄ exhibit a saturated value of ~ 2.0 for $\chi_{J_z}(\tau)$ at $\tau \rightarrow \beta/2$, indicating that the U-5*f* electrons are localized (not completely screened) and thus a frozen magnetic moment is present. Figure 3 (d) shows that the frozen magnetic moment of USbSe does not vanish entirely before the ferromagnetic transition upon cooling. Our research reveal that UTe₂ under pressure and USbSe are in the coherent regime. Notably, USbSe exhibits Pauli-type behavior and a local magnetic moment at low temperature, indicating a dual character of the U-5*f* electrons, with both localization and itinerancy present.

Duality driven by momentum dependent f-d hybridization. We sought to identify the origin of the duality by calculating orbital-projected values. The six partially occupied U-5*f* orbitals can be divided into three distinct groups, $f_\alpha = \{f_1, f_6\}$, $f_\beta = \{f_2, f_5\}$ and $f_\gamma = \{f_3, f_4\}$, based on their self-energy and hybridization functions, as illustrated in Fig.S3. Fig. 4 (a) displays the DOS, self-energies, and hybridization functions for f_1 and f_3 , which correspond to f_α and f_γ , respectively. Fig. 4 (b) shows the quasi-particle weight, $Z = 1/(1 - \frac{\partial \Sigma(i\omega)}{\partial i\omega})$.

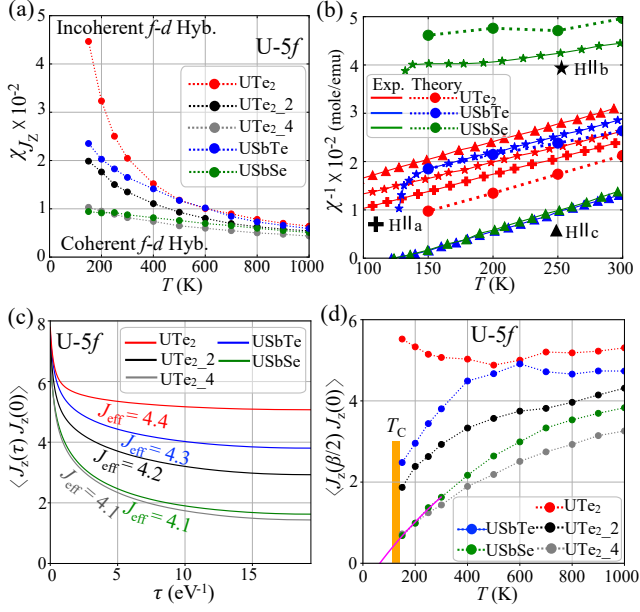


FIG. 3. (a) Calculated local total angular momentum susceptibility. (b) Comparison of inverse of magnetic susceptibility between calculations and experiments [7, 40]. (c) Local angular momentum correlation functions in the imaginary time τ . Calculated instantaneous J are presented with corresponding colors. (d) Temperature dependent frozen magnetic moments. The bar shows the ferromagnetic transition temperature $T_c = 127$ K of USbTe and USbSe [7].

Fig. 4 (c) shows α from the fitting of $\text{Im}\Sigma(i\omega_n) \simeq -T + A(i\omega_n)^\alpha$. Deviation from the linear variation, i.e., non-Fermi liquid behavior, can be attributed to the freezing of localized spin moments [44]. The DOS, self-energy, hybridization function, Z and α for partially occupied six f orbitals of all compounds were presented in Fig.S3, S4 and S5.

Figure 4 illustrates that UTe_2 has a higher Z factor than other compounds at elevated temperatures, implying a feeble electron correlation and consequently a small quasi particle peak near the Fermi level. As the temperature is decreased, the Z factor decreases due to the emergence of incoherent f - d Kondo hybridization and a large f DOS in the vicinity of the Fermi level [35], as shown in Fig. 4 (a) and (b). UTe_2 also has a smaller α value compared to other materials, which is attributed to its more pronounced frozen magnetic moments.

Figure 4 shows that UTe_{2_4} and USbSe , which are in the coherent regime, have larger α values than UTe_2 , indicating smaller magnetic moments. At temperatures below 300 K, the Z factors of UTe_{2_4} and USbSe are larger than that of UTe_2 , indicating a suppression of electron correlations and an increase in the coherence energy of the electrons. This suggests a transition from an incoherent to a coherent behavior, from Curie-like to Pauli-like, at low temperatures [41]. The transition is characterized by coherent f - d hybridization, resulting in an increased quasi-particle peak near the Fermi level. In contrast to UTe_2 , UTe_{2_4} and USbSe exhibit orbital selective hybridization. The hybridization function of f_3 at the Fermi level displays strong divergence in contrast to f_1 . This results

in a two peak structure of the DOS in the vicinity of the Fermi level, unlike the DOS of f_1 , as shown in Fig. 4 (a) and Fig.S6. This suggests that the degree of itinerancy is dependent on the orbital configuration. However, as shown in Fig. 4 (c) and Fig.S5, the orbital selective f - d hybridization does not have a significant effect on α for the six partially occupied f orbitals of USbSe . This indicates that the six f orbitals contribute similarly to the magnetic moment.

Figure 2 (e) shows the DOS of USbSe , which exhibits a kink in the vicinity of the Fermi level, indicating the presence of a VHS. This is due to the flat bands in the six partially occupied f projected spectral functions, as seen in Fig. 2 (f) and Fig.S7. The flat f bands are subject to coherent f - d hybridization, which is momentum dependent and forms partially flat bands along X-M- Γ and R-A-Z symmetry lines, resulting in the emergence of VHS. The momentum dependent f - d hybridization in uranium-based Kondo lattices gives rise to a dual character of Pauli-like magnetic susceptibility and local magnetic moments of U-5 f electrons in the coherent regime. This duality is reminiscent of the behavior of d electrons in Ni metallic systems, which act both as localized moments and itinerant contributions due to the VHS [28]. Our results show that all partially filled U-5 f orbitals contribute to local magnetic moments, which can be distinguished from OSMF to explain the dual nature. Table I and Fig. 2 demonstrate that the occupancy of U-5 f orbitals in the $J = 5/2$ multiplet is away from half filling, indicating that the U-5 f in the present compounds is not described by Mott-physics. This is further evidenced by the metallic U-5 f DOS shown in Fig. 2.

Investigating the magnetism of UTe_2 under pressure. To gain a better understanding of the origin of long-range magnetic ordering of UTe_2 at 1.5 GPa, we performed electronic structure calculations of UTe_2 in its orthorhombic phase with reduced volumes. It was demonstrated in the preceding section that UTe_2 with reduced volumes are in a coherent state. The temperature dependent χ_{J_z} shown in Fig. 3 (a) further supports the transition. The overall decrease in χ_{J_z} with decreasing volume is in agreement with the experimental observation of a decrease in χ_a under pressure [9]. Similar to USbSe , this coherent f - d hybridization transition does not affect all f bands in the reciprocal space, resulting in partially flat f bands depending on momentum. This results in the emergence of VHS from the flat U-5 f bands along the L-T-W and R-X₁-Z symmetry lines, as shown in Fig. 2 (c). Our findings suggest that UTe_2 is in a coherent state under pressure, with a VHS causing long-range magnetic ordering at low temperatures.

We discuss other potential causes of long-range magnetic ordering in two distinct scenarios of UTe_2 : fully-screened and under-screened. In the fully-screened case, the net local magnetic moment is zero. To induce long-range magnetic ordering, the local magnetic moment must appear. Fig. 3 (c) shows that the magnetic moment of U-5 f decreases with decreasing volume, which is in agreement with the experimental observation of a decrease in effective moments under pressure reported in Ref. [9]. Consequently, the reduced magnetic moment of U-5 f will remain fully-screened under pressure, with no impurities' magnetic moment to be coupled.

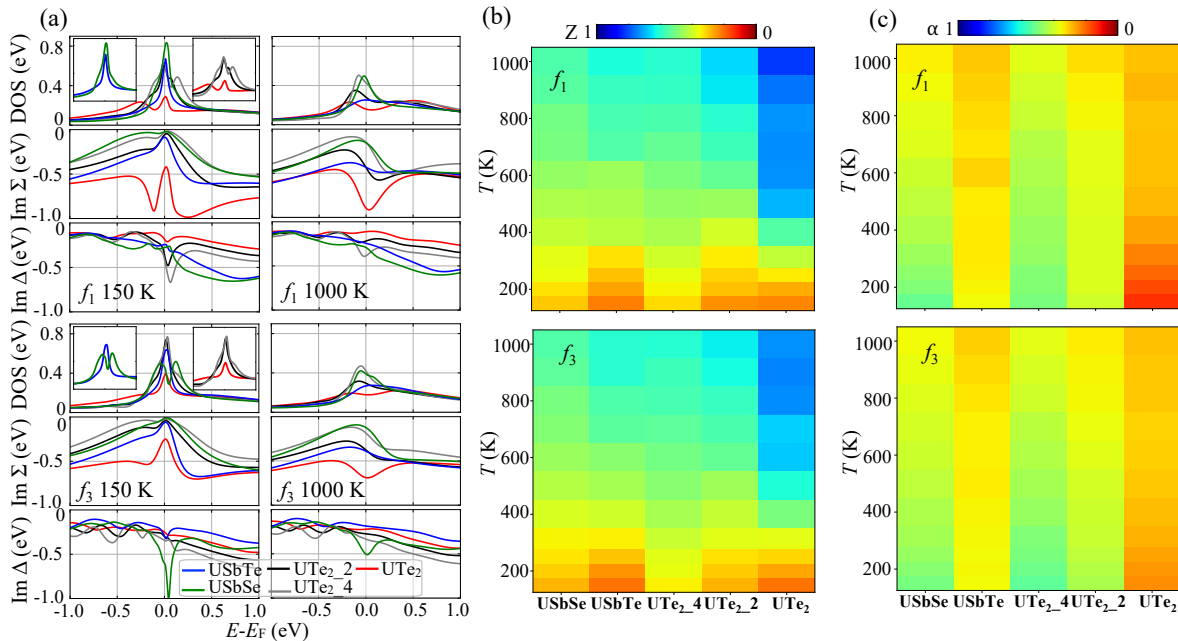


FIG. 4. (a) DOS, imaginary part of self-energies and hybridization functions for f_1 and f_3 . Temperature dependent of (b) the quasi-particle weight Z factors and (c) calculated α from the fitting of $\text{Im}\Sigma(i\omega_n) \simeq -\Gamma + A(i\omega_n)^\alpha$, for f_1 and f_3 . In (a), inset shows magnified views of DOS in the vicinity of the Fermi level.

In the case of under-screened UTe_2 , non-zero U-5*f* magnetic moments can interact through either exchange or RKKY interaction. It is reasonable to assume negligible direct exchange coupling between neighboring U-5*f* moments, as the f - f hybridization is negligible due to the small overlap of wave functions between U-5*f*. This is supported by our findings that f - d hybridization is dominant at low energy. We also suggest that RKKY interaction can be suppressed under pressure. Doniach's work [23] suggests that the transition from an antiferromagnetic to a Kondo-like state is driven by the competition between the binding energy of a Kondo singlet, $W_K \sim N(0)^{-1} e^{-1/N(0)J_0}$, and that of the RKKY antiferromagnetic state, $W_{AF} \sim J_0^2 N(0)$, where J_0 is exchange coupling constant between the localized moments and the conduction electrons and $N(0)$ is the density of conduction electron states. When J_0 is below a certain threshold, the RKKY state is the most prominent, while above this, the Kondo singlet binding is the most influential. The volume of UTe_2 was reduced, resulting in an increase in J_H of U-6*d* (see Fig. 1 (c)) due to the decrease in inter atomic distance. These results suggest that the RKKY interaction is weakened by increased J_0 under pressure on UTe_2 . Consequently, the RKKY interaction

is not a viable explanation for the emergence of long-range magnetic ordering in UTe_2 under pressure.

Conclusion. By altering the chemical composition or reducing the lattice parameters, uranium-based Kondo lattices are brought into a state of coherent f - d hybridization, thus giving rise to the emergence of Bloch-like quasiparticles from the renormalized U-5*f*, which in turn bring about a duality of Pauli-like susceptibility and local magnetic moments through the van Hove singularity. This novel perspective on the magnetic properties of the Kondo lattice provides a new theoretical basis to explain the mechanism of long-range magnetic ordering in Kondo lattices.

ACKNOWLEDGMENTS

We acknowledge the High Performance Computing Center (HPCC) at Texas Tech University for providing computational resources that have contributed to the research results reported within this paper. M.H.K was supported by faculty startup funds from Texas Tech University.

- [1] J. Schoenes, O. Vogt, J. Löhle, F. Hulliger, and K. Mattenberger, Variation of f -electron localization in diluted US and UTe, *Phys. Rev. B* **53**, 14987 (1996).
 [2] J. Lee, M. Matsuda, J. A. Mydosh, I. Zaliznyak, A. I. Kolesnikov, S. Süllow, J. P. Ruff, and G. E. Granroth, Dual na-

ture of magnetism in a uranium heavy-fermion system, *Phys. Rev. Lett.* **121**, 057201 (2018).

- [3] A. Amorese, M. Sundermann, B. Leedahl, A. Marino, D. Takegami, H. Gretarsson, A. Gloskovskii, C. Schlueter, M. W. Haverkort, Y. Huang, *et al.*, From antiferromagnetic and

- hidden order to Pauli paramagnetism in UM_2Si_2 compounds with $5f$ electron duality, *Proc. Natl. Acad. Sci.* **117**, 30220 (2020).
- [4] A. Szytuła, M. Slaski, B. Dunlap, Z. Sungaila, and A. Umezawa, Transport and heat capacity properties of UFe_2Si_2 , *J. Magn. Magn. Mater.* **75**, 71 (1988).
- [5] H. Siddiquee, C. Broyles, E. Kotta, S. Liu, S. Peng, T. Kong, B. Kang, Q. Zhu, Y. Lee, L. Ke, *et al.*, Breakdown of the scaling relation of anomalous Hall effect in Kondo lattice ferromagnet $USbTe$, *Nat. Commun.* **14**, 527 (2023).
- [6] D. Aoki, J.-P. Brison, J. Flouquet, K. Ishida, G. Knebel, Y. Tokunaga, and Y. Yanase, Unconventional superconductivity in UTe_2 , *J. Phys.: Condens. Matter* **34**, 243002 (2022).
- [7] D. Kaczorowski, H. Noël, and A. Zygmunt, Magnetic studies on UXY ($X = P, Sb$; $Y = Se, Te$) single crystals, *J. Magn. Magn. Mater.* **140**, 1431 (1995).
- [8] S. Thomas, F. Santos, M. Christensen, T. Asaba, F. Ronning, J. Thompson, E. Bauer, R. Fernandes, G. Fabbris, and P. Rosa, Evidence for a pressure-induced antiferromagnetic quantum critical point in intermediate-valence UTe_2 , *Sci. Adv.* **6**, eabc8709 (2020).
- [9] D. Li, A. Nakamura, F. Honda, Y. J. Sato, Y. Homma, Y. Shimizu, J. Ishizuka, Y. Yanase, G. Knebel, J. Flouquet, *et al.*, Magnetic properties under pressure in novel spin-triplet superconductor UTe_2 , *J. Phys. Soc. Jpn.* **90**, 073703 (2021).
- [10] D. Braithwaite, M. Vališka, G. Knebel, G. Lapertot, J.-P. Brison, A. Pourret, M. Zhitomirsky, J. Flouquet, F. Honda, and D. Aoki, Multiple superconducting phases in a nearly ferromagnetic system, *Commun. Phys.* **2**, 147 (2019).
- [11] S. Ran, H. Kim, I.-L. Liu, S. R. Saha, I. Hayes, T. Metz, Y. S. Eo, J. Paglione, and N. P. Butch, Enhancement and reentrance of spin triplet superconductivity in UTe_2 under pressure, *Phys. Rev. B* **101**, 140503 (2020).
- [12] V. Anisimov, I. Nekrasov, D. Kondakov, T. Rice, and M. Sigrist, Orbital-selective Mott-insulator transition in $Ca_{2-x}Sr_xRuO_4$, *Eur. Phys. J. B* **25**, 191 (2002).
- [13] E. A. Stepanov, Eliminating orbital selectivity from the metal-insulator transition by strong magnetic fluctuations, *Phys. Rev. Lett.* **129**, 096404 (2022).
- [14] F. B. Kugler and G. Kotliar, Is the orbital-selective mott phase stable against interorbital hopping?, *Phys. Rev. Lett.* **129**, 096403 (2022).
- [15] M. Kim, H.-S. Kim, K. Haule, and D. Vanderbilt, Orbital-selective Mott phase and non-Fermi liquid in $FePS_3$, *Phys. Rev. B* **105**, L041108 (2022).
- [16] B. Kang, H. Kim, Q. Zhu, and C. H. Park, Impact of f - d Kondo cloud on superconductivity of nickelates, *Cell Rep. Phys. Sci.* **4**, 101325 (2023).
- [17] L. M. Sandratskii, V. M. Silkin, and L. Havela, Entangled origins of the nonmagnetic states of U and Fe atoms in hydrogenated $UFeGe$, *Phys. Rev. Mater.* **7**, 024414 (2023).
- [18] P. Schlottmann and P. Sacramento, Multichannel Kondo problem and some applications, *Adv. Phys.* **42**, 641 (1993).
- [19] P. Nozieres and A. Blandin, Kondo effect in real metals, *J. Phys. France* **41**, 193 (1980).
- [20] N. B. Perkins, M. Nunez-Regueiro, B. Coqblin, and J. R. Iglesias, Underscreened Kondo lattice model applied to heavy fermion uranium compounds, *Phys. Rev. B* **76**, 125101 (2007).
- [21] C. Thomas, A. S. da Rosa Simoes, J. Iglesias, C. Lacroix, N. Perkins, and B. Coqblin, Application of the $S=1$ underscreened Anderson lattice model to Kondo uranium and neptunium compounds, *Phys. Rev. B* **83**, 014415 (2011).
- [22] H. v. Löhneysen, A. Rosch, M. Vojta, and P. Wölfle, Fermi-liquid instabilities at magnetic quantum phase transitions, *Rev. Mod. Phys.* **79**, 1015 (2007).
- [23] S. Doniach, The kondo lattice and weak antiferromagnetism, *physica B+C* **91**, 231 (1977).
- [24] L. Van Hove, The occurrence of singularities in the elastic frequency distribution of a crystal, *Phys. Rev.* **89**, 1189 (1953).
- [25] M. Fleck, A. M. Oleś, and L. Hedin, Magnetic phases near the Van Hove singularity in s - and d -band Hubbard models, *Phys. Rev. B* **56**, 3159 (1997).
- [26] R. Hlubina, S. Sorella, and F. Guinea, Ferromagnetism in the two dimensional t - t' Hubbard model at the van hove density, *Phys. Rev. Lett.* **78**, 1343 (1997).
- [27] H. Lin and J. Hirsch, Two-dimensional hubbard model with nearest- and next-nearest-neighbor hopping, *Phys. Rev. B* **35**, 3359 (1987).
- [28] A. Hausoel, M. Karolak, E. Şaşoğlu, A. Lichtenstein, K. Held, A. Katanin, A. Toschi, and G. Sangiovanni, Local magnetic moments in iron and nickel at ambient and earth's core conditions, *Nat. Commun.* **8**, 16062 (2017).
- [29] Y.-W. Liu, J.-B. Qiao, C. Yan, Y. Zhang, S.-Y. Li, and L. He, Magnetism near half-filling of a van hove singularity in twisted graphene bilayer, *Phys. Rev. B* **99**, 201408 (2019).
- [30] S. Ikeda, H. Sakai, D. Aoki, Y. Homma, E. Yamamoto, A. Nakamura, Y. Shiokawa, Y. Haga, and Y. Ōnuki, Single crystal growth and magnetic properties of UTe_2 , *J. Phys. Soc. Jpn.* **75**, 116 (2006).
- [31] F. Hulliger, New ternary thorium and uranium compounds MYX , *J. less-common met.* **16**, 113 (1968).
- [32] F. Aryasetiawan, M. Imada, A. Georges, G. Kotliar, S. Biermann, and A. I. Lichtenstein, Frequency-dependent local interactions and low-energy effective models from electronic structure calculations, *Phys. Rev. B* **70**, 195104 (2004).
- [33] S. Choi, P. Semon, B. Kang, A. Kutepov, and G. Kotliar, ComDMFT: A massively parallel computer package for the electronic structure of correlated-electron systems, *Comput. Phys. Commun.* **244**, 277 (2019).
- [34] K. Stöwe, Uncommon valence states in the metallic lanthanide and actinide diiodides MI_2 ($M=La, Ce, Nd, Gd$ and Th) and in the uranium tellurides UTe_2 , U_2Te_5 and ute_3 part 2: The uranium tellurides UTe_2 , U_2Te_5 and α - UTe_3 , *J. Alloys Compd.* **246**, 111 (1997).
- [35] B. Kang, S. Choi, and H. Kim, Orbital selective Kondo effect in heavy fermion superconductor UTe_2 , *npj Quantum Mater.* **7**, 64 (2022).
- [36] H. C. Choi, K. Haule, G. Kotliar, B. I. Min, and J. H. Shim, Observation of a kink during the formation of the Kondo resonance band in a heavy-fermion system, *Phys. Rev. B* **88**, 125111 (2013).
- [37] L. Jiao, S. Howard, S. Ran, Z. Wang, J. O. Rodriguez, M. Sigrist, Z. Wang, N. P. Butch, and V. Madhavan, Chiral superconductivity in heavy-fermion metal UTe_2 , *Nature* **579**, 523 (2020).
- [38] D. Kaczorowski, A. Pikul, and A. Zygmunt, Electrical transport properties of $USbSe$ and $USbTe$, *J. Alloys Compd.* **398**, L1 (2005).
- [39] S.-i. Fujimori, I. Kawasaki, Y. Takeda, H. Yamagami, A. Nakamura, Y. Homma, and D. Aoki, Electronic structure of UTe_2 studied by photoelectron spectroscopy, *J. Phys. Soc. Jpn.* **88**, 103701 (2019).
- [40] W. Knafo, M. Nardone, M. Vališka, A. Zitouni, G. Lapertot, D. Aoki, G. Knebel, and D. Braithwaite, Comparison of two superconducting phases induced by a magnetic field in UTe_2 , *Commun. Phys.* **4**, 40 (2021).
- [41] C. Marianetti, K. Haule, G. Kotliar, and M. Fluss, Electronic coherence in δ -Pu: A dynamical mean-field theory study, *Phys.*

- [Rev. Lett. **101**, 056403 \(2008\)](#).
- [42] A. Freeman, J. Desclaux, G. Lander, and J. Faber Jr, Neutron magnetic form factors of uranium ions, [Phys. Rev. B **13**, 1168 \(1976\)](#).
- [43] A. Belozero, A. Katanin, and V. Anisimov, Transition from Pauli paramagnetism to Curie-Weiss behavior in vanadium, [Phys. Rev. B **107**, 035116 \(2023\)](#).
- [44] P. Werner, E. Gull, M. Troyer, and A. J. Millis, Spin freezing transition and non-Fermi-liquid self-energy in a three-orbital model, [Phys. Rev. Lett. **101**, 166405 \(2008\)](#).